Received: 10 December 2018 | Accepted: 7 April 2019

DOI: 10.1111/1365-2435.13348

RESEARCH ARTICLE

Functional Ecology | BRITISH ECOLOGICAL SOCIETY

Warming increases the cost of growth in a model vertebrate

Diego R. Barneche | Miki Jahn | Frank Seebacher

School of Life and Environmental Sciences, The University of Sydney, Camperdown, New South Wales, Australia

Correspondence
Diego R. Barneche
Email: d.barneche@exeter.ac.uk

Present address
Diego R. Barneche, College of Life and Environmental Sciences, University of Exeter, Penryn, Cornwall, UK

Funding information
Australian Research Council (ARC), Grant/Award Number: DP180103036

Handling Editor: Isabel Smallegange

Abstract

1. Growth rates directly influence individual fitness and constrain the flow of energy within food webs. Determining what factors alter the energetic cost of growth is therefore fundamental to ecological and evolutionary models.
2. Here, we used theory to derive predictions about how the cost of growth varies over ontogeny and with temperature. We tested these predictions by measuring resting oxygen consumption and growth rates of zebrafish (*Danio rerio*) at four temperature treatments (20°C, 26°C, 29°C, 32°C). We calibrated oxygen consumption for ATP production by measuring the efficiency of mitochondria (P/O ratios) at the end of the experiment.
3. We show that, when compared to growth rates, rates of resting oxygen consumption exhibited a significantly higher temperature dependence and significantly lower mass scaling. P/O ratios varied substantially among individuals, but did not account for the observed difference in temperature dependence between rates. Consequently, the cost of growth was significantly higher at earlier ontogenetic stages, and it increased twofold between 20°C and 32°C. Temperature systematically decreased the size of adults between 26°C and 32°C.
4. To the best of our knowledge, our study represents the first attempt to characterise how the cost of growth varies over ontogeny and across temperatures in a model vertebrate. Rising temperatures will substantially alter the structure of ecosystems and the distribution of biomass in food webs because they drive a decline in the average size of individuals, and because higher costs of growth lead to inefficient energy transfer between trophic levels.

KEYWORDS
biomass, climate change, cost of growth, *Danio rerio*, efficiency, mitochondria, proton leakage, zebrafish

1 | INTRODUCTION

Growth is relevant to ecology across all levels of biological organisation. Through biosynthesis, individuals may acquire better competitive and reproductive abilities within a population, such that maximising growth rate can be of selective advantage (e.g. Sibly, Kodric-Brown, Luna, & Brown, 2018). Growth also represents the realised energy that can be transferred between trophic levels, and it therefore limits how sustainable trophic links are in food webs (Elton, 1927; Lindeman, 1942). Determining what causes growth to vary, and how much it costs energetically, constitutes a fundamental step in understanding how energy moves from individuals to ecosystems.

There is a lack in understanding about the physiological processes involved in energy allocation to growth within individuals. Energy derived from food is converted to chemical energy (adenosine

triphosphate, ATP) primarily in mitochondria. Energy is allocated to maintenance of cellular function and integrity, activity, growth and a substantial proportion may be lost as a result of inefficiency in the mitochondrial electron transport chain (Brand, 2005; Hulbert & Else, 2000). Therefore, the relative allocation of energy and the efficiency of ATP production are of fundamental importance because they can ultimately constrain trophic interactions. In human societies, for instance, understanding these energetic relationships will be key to enhance food security under future climates. In the particular case of fisheries, present-day changes in temperature are associated with changes in fish biomass production (O'Brien, Fox, Planque, & Casey, 2000), maturation schedules (Audzijonyte et al., 2018) and adult body sizes (van Rijn, Buba, DeLong, Kiflawi, & Belmaker, 2017). Of particular relevance is the fact that higher temperatures are often correlated with declines in fish adult body size, and this is widely known as the temperature-size rule (Atkinson, 1994; Audzijonyte et al., 2018; Gardner, Peters, Kearney, Joseph, & Heinsohn, 2011).

Fish growth trajectories are well characterised empirically and are typically represented by a sigmoidal relationship where individuals grow quickly early in ontogeny up to an optimum after which growth rates decline to reach an asymptote (e.g. Houde, 1989; Morais & Bellwood, 2018). Surprisingly, we still know relatively little about how much chemical energy from resting metabolism is invested by an organism—hereafter the "cost of growth"—to move along this trajectory (Barneche & Allen, 2018). In particular, some theoretical models assume that the cost of growth is invariant throughout ontogeny and across temperatures (e.g. Gillooly, Charnov, West, Savage, & Brown, 2002; West, Brown, & Enquist, 2001). However, empirical evidence suggests that such costs may decrease with increasing age and increase with increasing temperature (Barneche & Allen, 2018; Bradford & Crowther, 2013; Sears, Kerkhoff, Messerman, & Itagaki, 2012).

Mitochondrial energy production efficiency and the effects of temperature are of particular importance in determining the cost of growth. In fishes, the temperature sensitivity of resting oxygen consumption rates is significantly higher than that of growth rates (Barneche & Allen, 2018). A corollary of this finding (see Theory below) is that the cost of growth increases with temperature. An unresolved question is how much of this positive temperature dependence reflects actual increased ATP production and how much is owing to decreased mitochondrial efficiency.

Metabolic rate is most commonly measured as oxygen consumption. Ecological studies frequently assume that the fraction of ATP generated per oxygen atom consumed by mitochondria during substrate oxidation (P/O ratio) is constant. However, this is not necessarily the case, and P/O ratios may differ between individuals and can be influenced by environmental factors such as diet and temperature (Brand, 2005; Salin, Auer, Rey, Selman, & Metcalfe, 2015). As a result, the cost of growth of individuals and body mass accumulation may be context dependent and indirect evidence suggesting that cost of growth is temperature dependent (Barneche & Allen, 2018) must be confirmed by calibrating oxygen consumption for ATP production. Our current understanding of the effects of temperature on the cost of growth in ectotherms is primarily based on disparate compilations of data from the literature (e.g. Barneche & Allen, 2018; Moses et al., 2008; Wieser, 1994) where measurements of growth and oxygen consumption as a function of temperature are rarely made on the same populations and in the same experiment (e.g. Sears et al., 2012).

Our aim was to determine whether cost of growth and mitochondrial efficiency vary with temperature. We present an experimental approach guided by mathematical theory to measure the cost of growth in juvenile zebrafish (*Danio rerio*). We measured resting rates of oxygen consumption and growth rates weekly in individuals reared at different temperatures. We then measured mitochondrial efficiency in these same individuals at the end of the experiment to calibrate oxygen consumption rates for energy production. We tested five hypotheses: H1: Cost of growth is invariant over ontogeny; H2: Cost of growth is temperature dependent; H3: Individual asymptotic mass decreases at higher temperatures; H4: P/O ratios are temperature dependent; H5: P/O ratios are mass independent. We provide details of these hypotheses below.

2 | MATERIALS AND METHODS

2.1 | Theory and hypotheses

2.1.1 | A generalised growth model

Our experimental approach is guided by the generalised Pütter growth model (Pütter, 1920) for an organism with a wet mass of m (in g) with a growth rate per unit time, t (in days), of dm/dt (g/day),

$$\frac{dm}{dt} = am^{\theta} - bm, \tag{1}$$

where a (g $g^{-\theta}$ day^{-1}) and b (day^{-1}) are normalisation constants, and θ is a dimensionless mass-scaling exponent that generally takes a value within the 0.5–0.9 range (Glazier, 2005; Moses et al., 2008; von Bertalanffy, 1938). The mass-scaling exponent of the second term is commonly assumed to be 1 in multiple realisations of the generalised Pütter growth model (Moses et al., 2008; Ricklefs, 2003; von Bertalanffy, 1938; West et al., 2001). By definition, growth ceases when the organism reaches its asymptotic mass, M, that is $dm/dt = 0$, and therefore,

$$b = aM^{\theta-1}, \tag{2}$$

meaning that the constant b is functionally dependent on M. Substituting b into equation 1, we obtain a new expression for growth rates:

$$\frac{dm}{dt} = am^{\theta}\left[1 - \left(\frac{m}{M}\right)^{1-\theta}\right]. \tag{3}$$

The integral of equation 3 with respect to time yields an explicit expression for the mass of an individual, $m(t)$, at time t,

$$m(t) = M\left(1-\left(1-\left(\frac{m_0}{M}\right)^{1-\theta}\right)e^{-a(1-\theta)tM^{(\theta-1)}}\right)^{1/(1-\theta)} \approx M\left(1-e^{-a(1-\theta)tM^{(\theta-1)}}\right)^{1/(1-\theta)}, \quad (4)$$

where m_0 is the mass at hatching (t = 0); note that for the purposes of simplification, m_0 is here considered negligible with respect to the asymptotic mass, such that $m_0/M \approx 0$. Growth rates are generally measured experimentally by tracking individual mass increments over time, (i.e. $m(t)$), hence equation 4 can be used to estimate θ, a and M empirically when mass-at-age data are available.

2.1.2 | An energy based Pütter-like model

Recently, Barneche and Allen (2018) used the Ontogenetic Growth Model (OGM) of West et al. (2001), which is based on mass and energy balance, to investigate interspecific patterns of growth rates across multiple clades of fishes. The OGM has the same mathematical structure of Pütter's generalised model, although it differs philosophically in the meaning of its parameters. Specifically, the OGM assumes that the energy that an organism of mass m spends on growth is equal to the difference between resting metabolic rate, B_r (J/day), and maintenance cost, $B_m m$ (J/day):

$$E_m\frac{dm}{dt} = B_r - B_m m, \quad (5)$$

where E_m (J/g) is the cost of growth which comprises energy allocated to growth via both direct (e.g. cellular biosynthesis) and indirect (e.g. costs of digestion) paths (Clarke, 2019; Hou et al., 2008). According to West et al. (2001),

$$B_r = B_o m^{\alpha}, \quad (6)$$

and

$$B_m = B_o M^{\alpha-1}, \quad (7)$$

where B_o (J $g^{-\alpha}$ day^{-1}) is a metabolic normalisation constant that is independent from body mass, and α is a dimensionless mass-scaling exponent. Substituting equations 6 and 7 into equation 5 yields

$$\frac{dm}{dt} = \frac{B_o}{E_m}m^{\alpha}\left[1-\left(\frac{m}{M}\right)^{1-\alpha}\right], \quad (8)$$

which is mathematically identical to equation 3 when $a = B_o/E_m$ and $\alpha = \theta$. In the OGM, the expression $[1 - (m/M)^{1-\alpha}]$ represents the fraction of resting metabolic rate that is allocated to growth. Rearranging equation 8 yields and expression for the cost of growth:

$$E_m = \frac{B_r}{dm/dt}\left[1-\left(\frac{m}{M}\right)^{1-\alpha}\right]. \quad (9)$$

2.1.3 | Hypotheses

The hypotheses we test emerge from theory outlined above, and testing these hypotheses simultaneously will reveal the extent to which body mass and environmental temperatures affect the cost of growth.

Hypothesis H1: Cost of growth (E_m) is invariant over ontogeny

Experimentally, the cost of growth can be calculated by substituting dm/dt in equation 9 with equation 3 when mass-at-age and resting metabolic rate data are measured in parallel:

$$E_m = \frac{B_o m^{\alpha}\left[1-\left(\frac{m}{M}\right)^{1-\alpha}\right]}{am^{\theta}\left[1-\left(\frac{m}{M}\right)^{1-\theta}\right]}. \quad (10)$$

Note that both numerator and denominator of equation 10 depend on the asymptotic mass, M, that is estimated from mass-at-age data using equation 4. The OGM assumes that $\alpha = \theta$ and therefore that the cost of growth is invariant over the ontogenetic trajectory of an individual, that is $E_m \propto m^{\alpha-\theta} \propto m^0$ (Moses et al., 2008; West et al., 2001). This assumption has been corroborated interspecifically (Barneche & Allen, 2018; Moses et al., 2008). Yet, tests of this assumption at the *individual* level (arguably the level of relevance to the theory) are less common. For example, an experiment done across larval stages of the moth *Manduca sexta* indicates that the cost of growth is higher early in ontogeny (Sears et al., 2012). To the best of our knowledge, however, similar tests are still lacking in vertebrates.

Hypothesis H2: Cost of growth (E_m) is temperature dependent

Typically, for a given body mass, the normalisation constants for resting metabolic rates, B_o, and growth rates, a, vary with taxa, life-history strategies and environmental temperature (Barneche & Allen, 2018; Barneche et al., 2014; Brown, Gillooly, Allen, Savage, & West, 2004; Gillooly, Brown, West, Savage, & Charnov, 2001; Gillooly et al., 2002; Killen, Atkinson, & Glazier, 2010). Within the range of temperatures that are normally experienced by an organism, the relationship between the normalisation constants, $B_o(T)$ and $a(T)$, and temperature, T (K), is generally parameterised using an exponential Boltzmann–Arrhenius equation:

$$a(T) = a_o(T_s)e^{E_g I(T)}, \quad (11)$$

$$B_o(T) = B_o(T_s)e^{E_r I(T)}, \quad (12)$$

where $a_o(T_s)$ (g $g^{-\theta}$ day^{-1}) and $B_o(T_s)$ (J $g^{-\alpha}$ day^{-1}) are normalisation constants that are independent from mass and temperature at some arbitrary standardised temperature, T_s (K), $I(T)$ is an inverse temperature (eV^{-1}), $\frac{1}{k}\left(\frac{1}{T_s} - \frac{1}{T}\right)$, k is the Boltzmann constant (8.62×10^{-5} eV/K), and E_g and E_r (eV) are "activation" energies for growth and metabolic rates, respectively (Barneche & Allen, 2018; Barneche et al., 2014; Gillooly et al., 2001, 2002). The OGM, as it follows from equation 8, assumes that the temperature dependence of growth rates is governed by the effects of temperature on the resting metabolic rate normalisation, $B_o(T)$, that is $E_r = E_g$ (Gillooly et al., 2002). The corollary of this assumption is that the cost of growth, E_m, is independent from temperature, that is $E_m \propto e^{(E_r - E_g) \times I(T)} \propto e^0$. Barneche and Allen (2018) have challenged this assumption via a meta-analysis across 13 families of fishes, which indicated that E_m increases 22-fold between 0°C and 30°C. Although not directly comparable, these results might be consistent with evidence showing lower bacterial growth efficiency and lower plant carbon use efficiency at warmer temperatures (Apple, del Giorgio, & Kemp, 2006; Bradford & Crowther, 2013). However, similarly to hypothesis H1 above, hypothesis H2 remains to be tested at the individual level for a model vertebrate. Empirically, this hypothesis can be tested readily by comparing estimates of E_r and E_g.

Hypothesis H3: Individual asymptotic mass, $M(T)$, decreases at higher temperatures

Perhaps one of the most common macroecological patterns among ectothermic organisms is the "temperature-size rule," which states that maximum body sizes decrease at higher temperatures (Atkinson, 1994). Although this pattern has been observed within species experimentally, and across species via meta-analyses (reviewed in Atkinson, 1994; Gardner et al., 2011), the ubiquity and underlying mechanisms behind it are still debatable (see recent review in Audzijonyte et al., 2018). Here, we test this assumption empirically by fitting a Boltzmann–Arrhenius function to the $M(T)$ in equation 4:

$$M(T) = M_o(T_s)e^{E_s I(T)}, \quad (13)$$

where $M_o(T_s)$ (g) is a normalisation constant that is independent from temperature at some arbitrary standardised temperature, T_s (K), and E_s (eV) is an activation energy that dictates whether M changes with temperature. With this parameterisation, the temperature-size rule will be manifested if $E_s < 0$.

Mitochondria provide most of the ATP used to fuel biochemical reactions and biosynthesis. Metabolic rates measured as whole-organism oxygen consumption represent the underlying mitochondrial activity. A common assumption underlying oxygen consumption measurements is that there is a constant ratio between amount of ATP produced per atom of oxygen used (P/O ratio). However, this is not necessarily the case and, as we pointed out in the introduction, P/O ratios may vary between individuals and with environmental context, such as different temperatures (Brand, 2005; Salin et al., 2015).

Hypothesis H4: P/O ratios are temperature dependent

If increasing temperature decreases mitochondrial efficiency, that is, decreases P/O ratios (Salin et al., 2015), then organisms at higher temperatures need to respire more oxygen to maintain ATP production. Consequently, oxygen consumption rates may exhibit a greater temperature dependence compared to growth rates (Barneche & Allen, 2018).

Hypothesis H5: P/O ratios are mass independent

If growth and resting oxygen consumption rates exhibit the same mass scaling, it follows that the cost of growth should be mass independent. This is consistent with a previous meta-analysis on the interspecific cost of growth in fishes (Barneche & Allen, 2018). However, within species, there may be substantial difference between these scaling parameters (Sears et al., 2012), which could be explained by differences in mitochondrial efficiency (P/O ratios) between individuals of different mass.

2.2 | Testing hypotheses

2.2.1 | H1–H3

The size and temperature dependence of growth rates were estimated by combining equations (4), (11) and (13), and fitting this new expression to log-transformed data,

$$\ln m(t) = \ln M_o(T_s) + E_s I(T) + \frac{1}{1-\theta} \ln\left(1 - e^{-a_o(T_s)e^{E_g I(T)}(1-\theta)t(M_o(T_s)e^{E_s I(T)})^{(\theta-1)}}\right). \quad (14)$$

We fitted equation 14 using a Bayesian procedure implemented in the R package *brms* version 2.8.0 (Bürkner, 2017) in order to derive posterior distributions and associated 95% credible intervals (CIs) for the fitted parameters (Table S1). Because individual-level mass-at-age data constitutes a repeated measures design, we fitted equation 14 using a hierarchical modelling approach with individual-level random effects on $M_o(T_s)$, $a_o(T_s)$ and θ (Supporting Information). It is important to note that parameters E_s and E_g constitute fixed effects across individuals because individuals were reared at constant temperatures.

The size and temperature dependence of rates of oxygen consumption at rest were estimated by combining equations 6 and 12, and log-transforming data,

$$\ln B_r = \ln B_o(T_s) + E_r I(T) + \alpha \ln m. \quad (15)$$

Similar to equation 14 above, we fit equation 15 using a hierarchical modelling approach with individual-level random effects on $B_o(T_s)$ and α, but not for E_r (Supporting Information). Parameter estimates are presented in Table S2. In the Supporting Information, we also present results using a nonlinear parameterisation for $I(T)$ following Barneche et al. (2014).

After substituting a and B_o in equation 10 with the expressions in equations 11 and 12 respectively, calculations of E_m were performed based on within-individual parameter estimates of $B_o(T_s)$, $a_o(T_s)$, α and θ (from random effects) combined with across-individual parameter estimates for E_r, E_s and E_g (from fixed effects).

2.2.2 | H4–H5

We estimated whether P/O ratios exhibit any mass or temperature dependence by fitting a Bayesian hierarchical regression between measured P/O ratios as a response, and mass (in grams) and temperature (in Celsius) as predictors, with tank number as a random effect on the intercept (Supporting Information). We refrain from fitting the model on the log scale, or from using a Boltzmann–Arrhenius type equation because there is no a priori expectation for the functional relationship between these variables.

We estimated the resting oxygen consumption rates for individuals at weeks 10–11 based on their masses measured immediately prior to mitochondrial respiration assays, and tank temperature, using individual-level parameter estimates of $B_o(T_s)$ and α (from random effects) combined with across-individual parameter estimates for E_r. These individual estimates were then converted to mM O_2/day and multiplied by their respective P/O ratios in order to estimate the rate of ATP production (mM ATP/day). We then recalculated E_m (expressed in ATP/g) by first estimating dm/dt (similar to oxygen consumption above, but first combining equations 3, 11 and 13, with estimates of $a_o(T_s)$, $M_o(T_s)$ θ, E_s and E_g), and then diving ATP production rates by dm/dt.

2.3 | Experimental system

2.3.1 | Model species and experimental design

We test hypotheses H1–H5 by measuring resting oxygen consumption rates, growth rates and P/O ratios in zebrafish (*Danio rerio*; Barneche, Jahn, & Seebacher, 2019). All experiments were performed with the approval of the University of Sydney Animal Ethics Committee (approval number 2017/1200). We reared individuals from eggs to 3.5 months of age, when most individuals had achieved sexual maturity. Eggs were obtained from 28 breeding groups (two females, one male) of adult zebrafish, which were maintained in tanks at 27.5°C. Before mating, breeding groups were kept in separate zebrafish breeding tanks (Tecniplast, Rydalmere, Australia) overnight with a transparent divider separating males from females. The dividers were removed in the morning, and fertilisation of eggs followed immediately after that. Eggs were collected and rinsed with EM3 medium (5 mM NaCl, 0.17 mM KCl, 0.33 mM $CaCl_2$, 0.33 mM $MgSO_4$, 5% methylene blue) and placed in 26 Petri dishes with EM3 medium, each containing approximately 50–100 eggs. Eggs were maintained at 27–27.5°C in controlled-temperature rooms, and every day we removed unfertilised eggs or dead embryos and replaced 50% of the E3 medium. After hatching (24–48 hr post-fertilisation), larvae were fed cultures of *Paramecium* sp. twice daily. E3 medium was progressively substituted by ultrapure water (Sartorius, Göttingen, Germany) to which we added 0.5 g/L of sea salt (Red Sea Aquatics Ltd, UK). At day 10, larvae were equally split among nine 2-l tanks filled with 120 mL water each (26–26.5°C), at a density of 25 larvae per tank. Water volume and aeration were maintained by a slow drip feed. Tank water was replaced daily (20%–30%) after removal of faeces and dead larvae. Larvae were fed ad libitum once daily with a combination of *Artemia salina* nauplii (from 24 hr post-hatching) and commercial spirulina powder for 4 weeks.

After 4 weeks, we measured body mass of 80 randomly picked fish by gently drying and placing individuals into tared weighing dishes on a balance (LA-120S, Sartorius, Australia) containing sufficient water for the fish to be covered. The same individuals were transferred to four temperature treatments (20°C, 26°C, 29°C and 32°C). Within each treatment, there were four 10-L tanks and five individuals per tank. Tanks were placed in a constant temperature room at 20°C, and all tanks were initially maintained at 26°C using aquarium heaters. The target temperatures were achieved by changing the tank temperatures at 3°C per day. Within each tank, individuals were each kept in mesh containers which allowed us to follow individuals while fish were still in olfactory and visual contact with each other. Individuals were fed to satiation once daily with a combination of dry commercial food (Wardley's Tropical Fish Flakes, Hartz Mountain Company, Secaucus, USA) and *Artemia salina* nauplii. Water volume and temperatures were monitored daily, and tanks were cleaned weekly. Two individuals from the 32°C treatment died during the first two weeks of treatment and were therefore excluded from the analysis. Another two (one from 32°C, one from 29°C) individuals died between weeks 7 and 8, but were maintained for data analysis.

2.3.2 | Rates of oxygen consumption and growth

Each week for 8 weeks, resting rates of oxygen consumption and growth rates were measured for each individual. Oxygen consumption rates were measured as described in Seebacher, Borg, Schlotfeldt, and Yan (2016). Rates of oxygen consumption (in ml/L) were transformed to Joules/day following standard conversions (Barneche & Allen, 2018). Following measurements of oxygen consumption, we measured the mass of each individual as described above. After measurements, fish were transferred back to their respective baskets and fed.

2.3.3 | Mitochondrial bioenergetics and P/O ratios

Within two weeks following final respirometry measurements, fish were anaesthetised with ethyl 3-aminobenzoate methanesulphonate (buffered MS-222 solution, 0.3 g/L; Sigma-Aldrich, Australia) and then euthanised by cervical dislocation. Mitochondrial respiration was measured in a stirred respiration chamber (Mitocell MT200; Strathkelvin Instruments), with a microelectrode (model 1302; Strathkelvin Instruments) connected to an oxygen meter (model 782; Strathkelvin Instruments). Measurements were conducted

according to published protocols (Dos Santos, Galina, & Da-Silva, 2013; Guderley & Seebacher, 2011). Mitochondria were extracted from skeletal muscle tissue (0.08–0.21 g) in nine volumes (v/m) of isolation buffer (140 mM/L KCl, 20 mM/L HEPES, 5 mM/L $MgCl_2$, 2 mM/L EGTA, 1 mM/L ATP, 0.5 g/L 1% fatty acid free bovine serum albumin, pH 7.0). Homogenised tissue was centrifuged at 1,400 *g* for 5 min and the supernatant was centrifuged at 9,000 *g* for 9 min at 4°C to extract mitochondria. The pellet was resuspended in assay buffer (110 mM/L sucrose, 60 mM/L KCl, 0.5 mM/L EGTA, 3 mM/L $MgCl_2$, 20 mM/L taurine, 10 mM/L KH_2PO_4, 10 mM/L HEPES, 0.5 g/L 1% fatty acid free bovine serum albumin, pH 7.1; 200 µl buffer per 0.1 g of tissue). We used 50 µl of suspended mitochondria for each assay and conducted measurements at the developmental temperature of each individual (20°C, 26°C, 29°C or 32°C). State II respiration was initiated after the addition of malate (final concentration = 5 mM/L) and pyruvate (final concentration = 2.5 mM/L). Following this, ADP (final concentration = 0.1 mM/L) was added to measure the maximal rate of substrate oxidation (state III respiration). Uncoupled state IV respiration was measured once all ADP had been phosphorylated, and we confirmed state IV rates by the addition of oligomycin (final concentration = 2–4 µg/ml). Finally, we added p-trifluoromethoxy carbonyl cyanide phenyl hydrazone (FCCP, final concentration = 0.5 µmol/L) to confirm the integrity of mitochondria (Brand & Nicholls, 2011). We used a Bradford assay (Sigma, Castle Hill, Australia) to determine the protein concentration of the isolated mitochondria samples spectrophotometrically using BSA as the standard (in a Ultraspec 2100 pro UV, GE Healthcare, Australia). Measurements of mitochondrial respiration were performed in 74 of the 76 individuals, because two samples were lost to equipment failure.

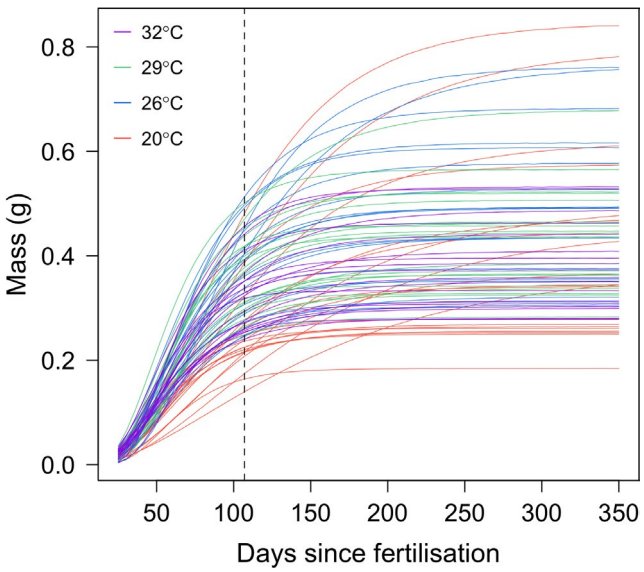

FIGURE 1 Model fits for individual-level growth curves, following equation 14. Vertical dashed line represents the average age of death, that is, when individuals had their mitochondrial respiration measured; fits thereafter serve the purpose of illustrating the model-estimates asymptotic masses. Colours represent the temperature treatments

3 | RESULTS

3.1 | Growth

Zebrafish individuals grew from 0.02 g (smallest) at the beginning of the temperature treatments to 0.58 g (largest) at the end of the experiment (Figure 1; see Figure S1 for individual-specific growth curves). Our growth model (equation 14) yielded an estimate for the mass scaling, θ, of 0.78 (95% Bayesian CI: 0.76–0.8). The estimate for the activation energy, E_g was 0.09 (CI: 0.02–0.16). After accounting for within-individual effects on the mass scaling (θ), growth normalisation constant ($\ln a_o(T_S)$) and asymptotic mass ($\ln M_o(T_S)$) normalisation constant, the model showed that growth rates varied 4.2-fold among individuals, indicated by the standard deviation of the growth normalisation constant, $\sigma_{\Delta \ln a_o(T_s)}$ ($\approx e^{2 \times 0.72}$, with $\sigma_{\Delta \ln a_o(T_s)} = 0.72$; Table S1).

The average asymptotic mass of zebrafish, $M(T)$, did not vary systematically with temperature, as parameterised by a Boltzmann–Arrhenius equation (Figure 2; equation 13; average E_s: 0.07; CI: −0.09 to 0.23). We observed a 2.0-fold variation in the temperature-independent asymptotic sizes, $\ln M_o(T_s)$, among individuals of zebrafish (i.e. $\approx e^{2 \times 0.35}$, with $\sigma_{\Delta \ln M_o(T_s)} = 0.35$; Table S1).

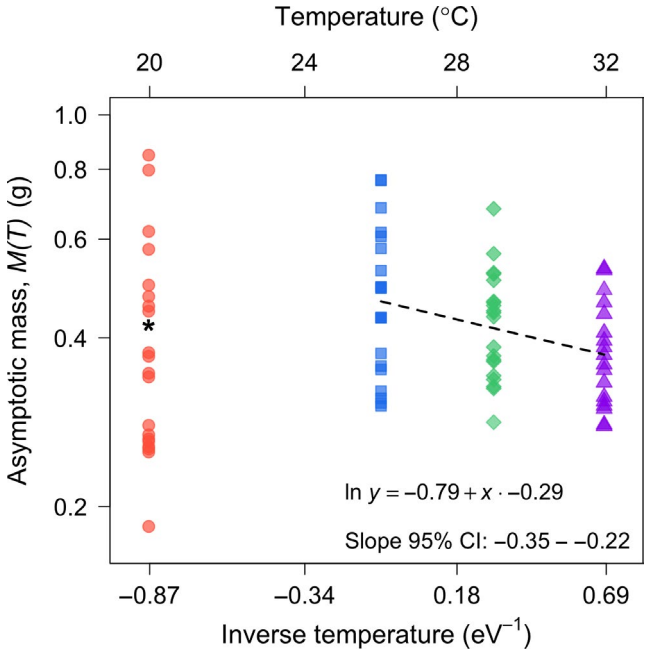

FIGURE 2 Relationship between asymptotic mass, $M(T)$ (equation 13) and temperature treatment, T. Values of $M(T)$ were estimated based on individual-level parameter estimates obtained from equation 14 using a Bayesian procedure. The dashed line and equation were obtained using a Bayesian linear model fit to the data between 26°C and 32°C (Supporting Information). Asterisk indicates the average $M(T)$ among individuals at 20°C. Slope 95% CI represent Bayesian credible intervals for the estimated slope. Points are equivalent to the end of individual growth trajectories in Figure 1

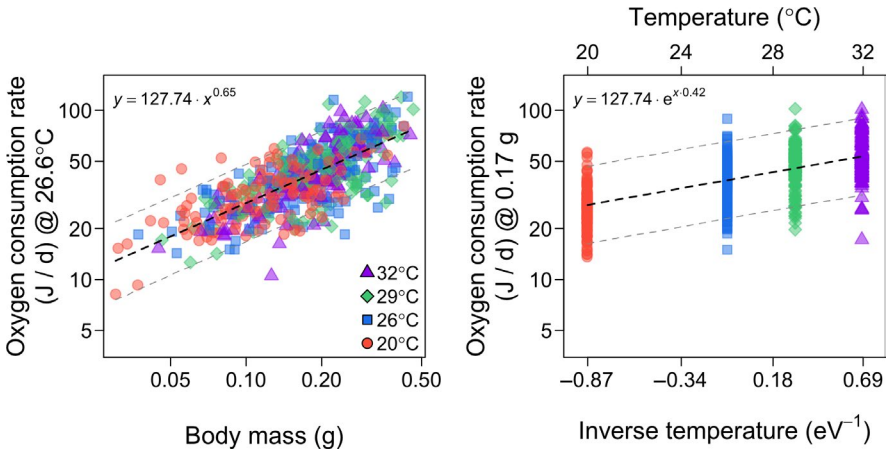

FIGURE 3 Zebrafish resting rates of oxygen consumption with respect to body mass (left) and temperature treatment (right). Parameter estimates (listed in Table S2) were obtained using Bayesian methods. The effect of temperature on oxygen consumption rate (left) was controlled for by standardising the temperature measures to T_s = 299.75 K (= 26.6°C) based on the Boltzmann relationship. The effect of body mass (right) was controlled for by standardising measures to 0.17 g based on the among-individuals mass-scaling exponent. The mass-corrected rate at temperature T_s corresponds to an average among individuals. Thick and thin dashed lines represent among-individuals model average fits and 95% Bayesian credible intervals respectively

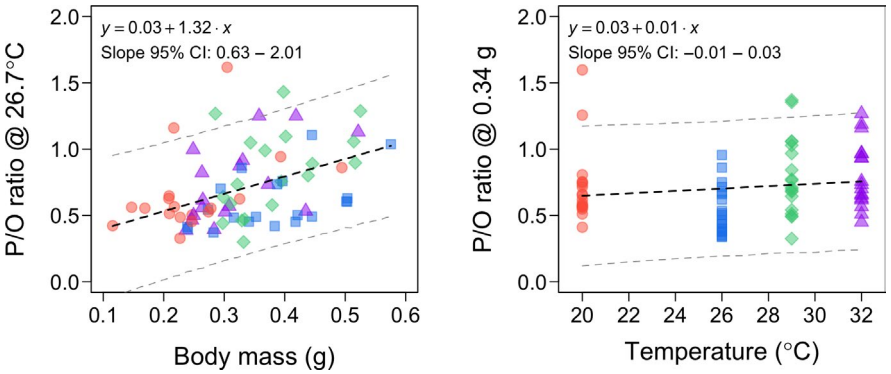

FIGURE 4 Zebrafish P/O ratios with respect to body mass (left) and temperature treatment (right). Parameter estimates (listed in Table S4) were obtained using Bayesian methods. The effect of temperature on P/O ratios (left) was controlled for by centralising the temperature measures to 26.7°C. The effect of body mass (right) was controlled for by standardising measures to 1.4 grams. Thick and thin dashed lines represent among-individuals model average fits and 95% Bayesian credible intervals, respectively. Colours and symbols represent different temperature treatments as per Figure 3a. Slope 95% CI represent Bayesian credible intervals for the estimated slope

3.2 | Oxygen consumption

The model for resting oxygen consumption rates (equation 15) yielded estimates for the mass scaling, α, of 0.65 (CI: 0.6–0.71), and an activation energy, E_r, of 0.42 (CI: 0.36–0.49; Figure 3, Table S2; see Figure S2 for individual-specific curves). After accounting for within-individual effects on the mass scaling (α), and normalisation constant (ln $B_o(T_s)$), the model revealed that rates of oxygen consumption vary by 1.9-fold among individuals (i.e. $\approx e^{2 \times 0.33}$, with $\sigma_{\Delta \ln B_o(T_s)}$ = 0.33; Table S2).

3.3 | Mitochondrial bioenergetics

P/O ratios did not show any systematic variation with temperature (average slope: 0.01; CI: −0.01 to 0.03), but showed a strong positive relationship with mass (average slope: 1.32; CI: 0.63–2.01; Figure 4). After accounting for within-tank effects on the intercept, the model revealed that P/O ratios varied 0.02-fold among tanks (i.e. $\approx 0.13^2$, with $\sigma_{\Delta \beta_0}$ = 0.13; Table S4).

4 | DISCUSSION

4.1 | Hypothesis H1: Cost of growth (E_m) is invariant over ontogeny

We reject hypothesis H1 because the average across-individuals mass-scaling slopes for growth (θ) and oxygen consumption (α) were substantially different from one another (judging by the non-overlap between CIs). Particularly, the fact that $\alpha - \theta = -0.13$ (Figure 5) indicates that the cost of growth, E_m, decreased with increasing mass of the individual following equation 10. This result is consistent with experimental evidence shown for larval moths, where biosyntheses costs were higher during earlier

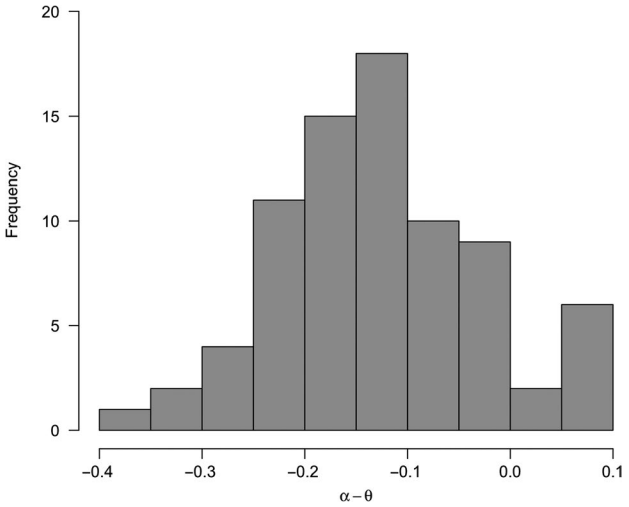

FIGURE 5 Distribution of the difference between within-individuals mass-scaling slopes for oxygen consumption (α) and growth (θ). Negative values indicate that the cost of growth, E_m, decreases with increasing mass of the individual following equation 10. Estimates of α and θ were obtained from individual-level random effects using equations 14 and 15 (See methods for full explanation)

developmental stages (Sears et al., 2012). Moreover, it suggests that the efficiency of ATP production increases as the animal grows (see hypothesis H5 below).

4.2 | Hypothesis H2: Cost of growth (E_m) is temperature dependent

Consistent with H2, the average across-individual activation energies for growth and oxygen consumption were substantially different from one another. Similar to patterns across species of fishes (Barneche & Allen, 2018), the cost of growth increased with temperature in zebrafish (i.e. $E_m \propto e^{(E_r - E_g) \times I(T)} \propto e^{0.33 \times I(T)}$). Particularly, it increased twofold across the range of our test temperatures. If other processes (e.g. active metabolic rates, assimilation rates and efficiency) are held fixed, higher costs of growth imply less efficient energy transfer between trophic levels (Barneche & Allen, 2018). Such inefficiency would be qualitatively consistent with evidence showing declines in carbon use efficiency—the amount of C used for growth relative to the amount of C that has been respired—in plants (Bradford & Crowther, 2013), and microbes (Apple et al., 2006; Manzoni, Taylor, Richter, Porporato, & Ågren, 2012) at higher temperatures. It is also consistent with experiments showing that the trophic discrimination, that is the difference in isotope values between consumers and their resource, is lower at warmer treatments in crickets (Cloyed, Eason, & Dell, 2018). Recent theory, combined with meta-analysis, indicates that product formation is more sensitive to temperature (equivalent to our E_r) changes than diffusion or transport processes (equivalent to our E_g; Ritchie, 2018) and potentially explains why efficiency of energy transfer (via the energetic cost of growth) might be lower at higher temperatures.

4.3 | Hypothesis H3: Individual asymptotic mass, $M(T)$, decreases at higher temperatures

We reject H3 because the average asymptotic (i.e. maximum) size of zebrafish, $M(T)$, did not vary systematically with temperature. However, this result seems primarily driven by the fact that the asymptotic size of fish at 20°C was smaller on average (asterisk on Figure 2) relative to what would be expected based on the temperature-size rule and exhibited considerable variation. For the three higher temperatures (26°C, 29°C and 32°C), a Bayesian linear model between ln M and inverse temperature, $I(T)$, yields a significant negative relationship (Figure 2; Supporting Information). This result suggests that 20°C may be compromising the growth

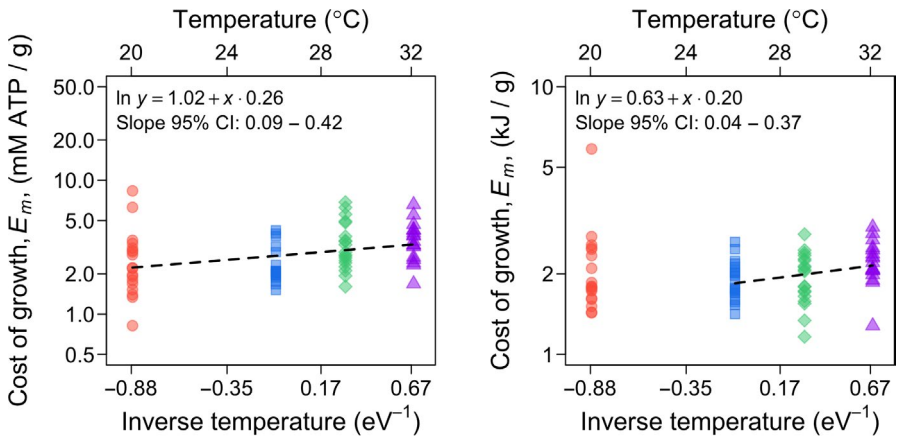

FIGURE 6 Relationship between the cost of growth, E_m (equation 10), and temperature treatment, T. These estimates were calculated for individuals at the end of the experiment, based on individual-level random effects from equations 14 and 15 (See methods for full explanation). Values on the left have been corrected for P/O ratios, whereas values on the right have not. The dashed lines and equations were obtained using Bayesian linear models (Supporting Information). Colours and symbols represent different temperature treatments as per Figure 3a. Slope 95% CI represent Bayesian credible intervals for the estimated slope

potential of this tropical species, perhaps because all individuals were bred at 26.5°C for a month before being transferred to their temperature treatments. The early developmental temperature (26.5°C) may have set phenotypes on a trajectory that is less cold-tolerant compared to fish bred at a lower temperature (e.g. Scott & Johnston, 2012). Hence, future studies should determine the effects of developmental and trans-generational effects on the cost of growth.

4.4 | Hypotheses H4: P/O ratios are temperature dependent, and H5: P/O ratios are mass independent

We reject hypotheses H4 and H5 because P/O ratios did not show any systematic variation with temperature, but showed a strong positive relationship with mass (Figure 4). The latter result potentially explains our rejection of hypothesis H1 because larger individuals consume less oxygen to produce the same amount of ATP. Estimates of E_m (mM ATP/g) obtained by combining individual-level P/O ratios with individual-level oxygen consumption reveal considerable among-individual variation (Figure 6a), particularly when compared to individual-level estimates of E_m (J/g) based on equation 10 (Figure 6b). Correcting oxygen consumption based on P/O ratios lends further support to hypothesis H2 (Figure 6a) and suggests that the among-individuals variation in E_m values in Figure 6b (estimated from oxygen consumption) masks the true relationship between E_m and temperature, and is primarily due to different levels of mitochondrial efficiency. We note also that, similarly to the findings for asymptotic body mass, the cost of growth in Figure 6b is positively correlated with temperature between 26°C and 32°C, but shows larger values at the cold temperature treatment. This reinforces the idea that the cold temperature treatment might be compromising physiological processes (here mitochondrial efficiency) in these individuals.

4.5 | General implications

The estimates for the mass scaling of growth rates, θ, were consistent with the 0.5–0.9 range generally reported for fishes; however, the estimate for the activation energy, E_g, was substantially shallower than the 0.3–0.7 eV range (Barneche & Allen, 2018; Gillooly et al., 2002). On the other hand, for oxygen consumption, both estimates for the mass scaling, α, and activation energy, E_r, were consistent with previously reported ranges (Barneche et al., 2014; Gillooly et al., 2001). We note though that α was substantially shallower than the canonical 3/4 that is generally reported among different species of fish (Barneche & Allen, 2018; Barneche et al., 2014; Gillooly et al., 2001). Rather, it was consistent with previous studies reporting an intraspecific mass-scaling exponent closer to 2/3 (Glazier, 2005; Killen et al., 2010). Importantly, this finding violates the assumption made in the original OGM, where the inter- and intraspecific mass-scaling exponents are assumed to be the same (Moses et al., 2008; West et al., 2001), and indicates that other mechanisms (e.g. lifestyle, temperature) may explain the variation in metabolic rates among species of similar relative age and mass (Killen et al., 2010).

Here, we present the first assessment of the mass and temperature dependence in the cost of growth for a model fish. In doing so, we reveal substantial variation among individuals and that small individuals at warmer temperatures exhibit higher costs of growth. This indicates that the cost of growth is a variable trait, and it should therefore be the focus of future studies in order to investigate both its underlying mechanisms, as well as the ecological variables and life-history strategies that cause it to vary. Our study emphasises that there are higher costs to growing in warmer environments. Everything else being constant, higher costs of growth lead to less efficient energy transfer between trophic levels. Thus, rising temperatures could alter the structure of ecosystems and the distribution of biomass in food webs through changes in individual-level growth dynamics.

ACKNOWLEDGEMENTS

We thank C.I. Miln, D.W.A. Noble, I. Loughland and P. Goncalves for support during the experiments and fish breeding. We also thank A.P. Allen for suggestions on theory presentation. This project was supported by Australian Research Council (ARC) Discovery Grant DP180103036 to F.S.

CONFLICT OF INTEREST

The authors declare no conflict of interest.

AUTHORS' CONTRIBUTIONS

D.R.B. and F.S. conceived the study; D.R.B. and M.J. conducted experiments; D.R.B. analysed the data and wrote the first version of the manuscript; and D.R.B. and F.S. edited the manuscript.

DATA ACCESSIBILITY

All data and R code (data manipulation, analyses, figures and tables) can be downloaded from a GitHub repository https://github.com/dbarneche/zebrafishCostOfGrowth (Barneche, Jahn, & Seebacher, 2019).

ORCID

Diego R. Barneche https://orcid.org/0000-0002-4568-2362

REFERENCES

Apple, J. K., del Giorgio, P. A., & Kemp, W. M. (2006). Temperature regulation of bacterial production, respiration, and growth efficiency in a temperate salt-marsh estuary. *Aquatic Microbial Ecology*, *43*, 243–254. https://doi.org/10.3354/ame043243

Atkinson, D. (1994). Temperature and organism size: A biological law for ectotherms? *Advances in Ecological Research*, *25*, 1–58.

Audzijonyte, A., Barneche, D. R., Baudron, A. R., Belmaker, J., Clark, T. D., Marshall, C. T., … van Rijn, I. (2018). Is oxygen limitation in warming waters a valid mechanism to explain decreased body sizes in aquatic ectotherms? *Global Ecology and Biogeography*, *28*, 64–77.

Barneche, D. R., & Allen, A. P. (2018). The energetics of fish growth and how it constrains food-web trophic structure. *Ecology Letters*, *21*, 836–844. https://doi.org/10.1111/ele.12947

Barneche, D. R., Jahn, M., & Seebacher, F. (2019). dbarneche/zebrafish-CostOfGrowth: Published version of paper data and code: Warming increases the cost of growth in a model vertebrate (Version v1.0.0). *Zenodo*. https://doi.org/10.5281/zenodo.2634100

Barneche, D. R., Kulbicki, M., Floeter, S. R., Friedlander, A. M., Maina, J., & Allen, A. P. (2014). Scaling metabolism from individuals to reef-fish communities at broad spatial scales. *Ecology Letters*, *17*, 1067–1076. https://doi.org/10.1111/ele.12309

Bradford, M. A., & Crowther, T. W. (2013). Carbon use efficiency and storage in terrestrial ecosystems. *New Phytologist*, *199*, 7–9. https://doi.org/10.1111/nph.12334

Brand, M. (2005). The efficiency and plasticity of mitochondrial energy transduction. *Biochemical Society Transactions*, *33*, 897–904. https://doi.org/10.1042/BST0330897

Brand, M. D., & Nicholls, D. G. (2011). Assessing mitochondrial dysfunction in cells. *Biochemical Journal*, *435*, 297–312. https://doi.org/10.1042/BJ20110162

Brown, J. H., Gillooly, J. F., Allen, A. P., Savage, V. M., & West, G. B. (2004). Toward a metabolic theory of ecology. *Ecology*, *85*, 1771–1789. https://doi.org/10.1890/03-9000

Bürkner, P. (2017). brms: An R package for Bayesian multilevel models using Stan. *Journal of Statistical Software*, *80*, 1–28.

Clarke, A. (2019). Energy flow in growth and production. *Trends in Ecology & Evolution*. https://doi.org/10.1016/j.tree.2019.02.003

Cloyed, C. S., Eason, P. K., & Dell, A. I. (2018). The thermal dependence of carbon stable isotope incorporation and trophic discrimination in the domestic cricket, *Acheta domesticus*. *Journal of Insect Physiology*, *107*, 34–40. https://doi.org/10.1016/j.jinsphys.2018.02.003

Dos Santos, R. S., Galina, A., & Da-Silva, W. S. (2013). Cold acclimation increases mitochondrial oxidative capacity without inducing mitochondrial uncoupling in goldfish white skeletal muscle. *Biology Open*, *2*, 82–87. https://doi.org/10.1242/bio.20122295

Elton, C. S. (1927). *Animal ecology*. New York, NY: Macmillan Co.

Gardner, J. L., Peters, A., Kearney, M. R., Joseph, L., & Heinsohn, R. (2011). Declining body size: A third universal response to warming? *Trends in Ecology & Evolution*, *26*, 285–291. https://doi.org/10.1016/j.tree.2011.03.005

Gillooly, J. F., Brown, J. H., West, G. B., Savage, V. M., & Charnov, E. L. (2001). Effects of size and temperature on metabolic rate. *Science*, *293*, 2248–2251. https://doi.org/10.1126/science.1061967

Gillooly, J. F., Charnov, E. L., West, G. B., Savage, V. M., & Brown, J. H. (2002). Effects of size and temperature on developmental time. *Nature*, *417*, 70–73. https://doi.org/10.1038/417070a

Glazier, D. S. (2005). Beyond the '3/4-power law': Variation in the intra-and interspecific scaling of metabolic rate in animals. *Biological Reviews*, *80*, 611–662. https://doi.org/10.1017/S1464793105006834

Guderley, H., & Seebacher, F. (2011). Thermal acclimation, mitochondrial capacities and organ metabolic profiles in a reptile (*Alligator mississippiensis*). *Journal of Comparative Physiology B*, *181*, 53–64. https://doi.org/10.1007/s00360-010-0499-1

Hou, C., Zuo, W., Moses, M. E., Woodruff, W. H., Brown, J. H., & West, G. B. (2008). Energy uptake and allocation during ontogeny. *Science*, *322*, 736–739. https://doi.org/10.1126/science.1162302

Houde, E. D. (1989). Comparative growth, mortality, and energetics of marine fish larvae: Temperature and implied latitudinal effects. *Fishery Bulletin*, *87*, 471–495.

Hulbert, A. J., & Else, P. L. (2000). Mechanisms underlying the cost of living in animals. *Annual Review of Physiology*, *62*, 207–235. https://doi.org/10.1146/annurev.physiol.62.1.207

Killen, S. S., Atkinson, D., & Glazier, D. S. (2010). The intraspecific scaling of metabolic rate with body mass in fishes depends on lifestyle and temperature. *Ecology Letters*, *13*, 184–193. https://doi.org/10.1111/j.1461-0248.2009.01415.x

Lindeman, R. L. (1942). The trophic-dynamic aspect of ecology. *Ecology*, *23*, 399–417. https://doi.org/10.2307/1930126

Manzoni, S., Taylor, P., Richter, A., Porporato, A., & Ågren, G. I. (2012). Environmental and stoichiometric controls on microbial carbon-use efficiency in soils. *New Phytologist*, *196*, 79–91. https://doi.org/10.1111/j.1469-8137.2012.04225.x

Morais, R. A., & Bellwood, D. R. (2018). Global drivers of reef fish growth. *Fish and Fisheries*, *19*, 874–889. https://doi.org/10.1111/faf.12297

Moses, M. E., Hou, C., Woodruff, W. H., West, G. B., Nekola, J. C., Zuo, W., & Brown, J. H. (2008). Revisiting a model of ontogenetic growth: Estimating model parameters from theory and data. *The American Naturalist*, *171*, 632–645. https://doi.org/10.1086/587073

O'Brien, C. M., Fox, C. J., Planque, B., & Casey, J. (2000). Climate variability and north sea cod. *Nature*, *404*, 142. https://doi.org/10.1038/35004654

Pütter, A. (1920). Wachstumähnlichkeiten. *Pflügers Archive für Gesamte Physiologie Menschen und Tiere*, *180*, 298–340. https://doi.org/10.1007/BF01755094

Ricklefs, R. E. (2003). Is rate of ontogenetic growth constrained by resource supply or tissue growth potential? A comment on West et al's model. *Functional Ecology*, *17*, 384–393. https://doi.org/10.1046/j.1365-2435.2003.00745.x

Ritchie, M. E. (2018). Reaction and diffusion thermodynamics explain optimal temperatures of biochemical reactions. *Scientific Reports*, *8*, 11105. https://doi.org/10.1038/s41598-018-28833-9

Salin, K., Auer, S. K., Rey, B., Selman, C., & Metcalfe, N. B. (2015). Variation in the link between oxygen consumption and ATP production, and its relevance for animal performance. *Proceedings of the Royal Society of London B: Biological Sciences*, *282*, 20151028.

Scott, G. R., & Johnston, I. A. (2012). Temperature during embryonic development has persistent effects on thermal acclimation capacity in zebrafish. *Proceedings of the National Academy of Sciences of the United States of America*, *109*, 14247–14252. https://doi.org/10.1073/pnas.1205012109

Sears, K. E., Kerkhoff, A. J., Messerman, A., & Itagaki, H. (2012). Ontogenetic scaling of metabolism, growth, and assimilation: Testing metabolic scaling theory with *Manduca sexta* larvae. *Physiological and Biochemical Zoology*, *85*, 159–173. https://doi.org/10.1086/664619

Seebacher, F., Borg, J., Schlotfeldt, K., & Yan, Z. (2016). Energetic cost determines voluntary movement speed only in familiar environments. *Journal of Experimental Biology*, *219*, 1625–1631. https://doi.org/10.1242/jeb.136689

Sibly, R. M., Kodric-Brown, A., Luna, S. M., & Brown, J. H. (2018). The shark-tuna dichotomy: Why tuna lay tiny eggs but sharks produce large offspring. *Royal Society Open Science*, *5*, 180453.

van Rijn, I., Buba, Y., DeLong, J., Kiflawi, M., & Belmaker, J. (2017). Large but uneven reduction in fish size across species in relation to changing sea temperatures. *Global Change Biology*, *23*, 3667–3674. https://doi.org/10.1111/gcb.13688

von Bertalanffy, L. (1938). A quantitative theory of organic growth (Inquiries on growth laws. II). *Human Biology*, *10*, 181–213.

West, G. B., Brown, J. H., & Enquist, B. J. (2001). A general model for ontogenetic growth. *Nature*, *413*, 628–631. https://doi.org/10.1038/35098076

Wieser, W. (1994). Cost of growth in cells and organisms: General rules and comparative aspects. *Biological Reviews*, *69*, 1–33. https://doi.org/10.1111/j.1469-185X.1994.tb01484.x

SUPPORTING INFORMATION

Additional supporting information may be found online in the Supporting Information section at the end of the article.

How to cite this article: Barneche DR, Jahn M, Seebacher F. Warming increases the cost of growth in a model vertebrate. *Funct Ecol*. 2019;33:1256–1266. https://doi.org/10.1111/1365-2435.13348